Particle dynamics and radiation in an ultra-intense standing wave

M. Jirka[1,2], O. Klimo[1,2], S. Weber[2], S. V. Bulanov[3], T. Zh. Esirkepov[3], E. G. Gelfer[4], S. S. Bulanov[5], G. Korn[2]

[1] *Faculty of Nuclear Sciences and Physical Engineering, Czech Technical University in Prague, Prague, Czech Republic*

[2] *Institute of Physics of the CAS, ELI-Beamlines project, Prague, Czech Republic*

[3] *National Institutes for Quantum and Radiological Science and Technology, Chiba , Japan*

[4] *National Research Nuclear Univ MEPhI, Moscow, Russia*

[5] *Lawrence Berkeley National Laboratory, Berkeley, California, USA*

As 10 PW laser facilities are now being built [1], more attention is paid to studying interactions at ultra-relativistic laser intensities of the order of 10^{23-24} W/cm^2. Such a high laser intensity will allow to enter the quantum dominated regime of the interaction in which prolific pair production via Breit-Wheeler process may occur. Therefore, possible future interaction scenarios leading to prolific gamma-ray emission and pair production in a strong electromagnetic (EM) field are studied now, such as interaction of charged particles with two or more counter-propagating laser beams [2, 3]. Using 2D PIC simulations we studied photon emission and pair production in the standing wave produced by two focused colliding laser pulses interacting with a target in their common focal spot. The influence of target density, thickness and material on gamma-ray generation and pair creation is assessed for both laser polarization.

There are two dimensionless parameters characterizing the interaction of a charged particle with the EM field. The classical nonlinearity parameter $a_0 = eE_0/m_e\omega_0 c$ measures the energy gain of an electron over the field wavelength in units of $2\pi m_e c^2$, where e and m_e are the electron charge and mass, E and ω_0 are EM field strength and frequency, c is the speed of light, respectively [4]. The interaction of electrons (photons) with the EM field is characterized by the parameter $\chi_e = [|(F_{\mu\nu}p_\nu)^2|]^{1/2}/m_e c E_S$ ($\chi_\gamma = [|(F_{\mu\nu}\hbar k_\nu)^2|]^{1/2}/m_e c E_S$), where $E_S = m_e^2 c^3/e\hbar \simeq 1.3\times 10^{18}$ V/m [5], $\hbar$ is the Planck constant, and $F_{\mu\nu}$ is the EM field tensor. As soon as $a_0 \gg 1, \chi_e > 1$ and $\chi_\gamma > 1$, the QED regime is entered and number of generated photons and electron-positron pairs exponentially grows [6].

We used the 2D version of the simulation code EPOCH [7] in which photon emission and pair production via Breit-Wheeler [8] process is implemented using Monte-Carlo method. We studied the interaction of circularly (CP) and linearly (LP) polarized colliding laser pulses with the target placed in their common focal spot. The laser pulse has Gaussian temporal profile of duration 30 fs FWHM, wavelength $\lambda = 1$ μm and intensity of 1.11×10^{24} W/cm^2 ($a_0 =$

900). The colliding laser pulses propagate along the x-axis and are focused to a focal spot of radius $w_0 = 1.5\lambda$. The circular target diameters are in the range of 0.5λ and 2λ having densities $0.05n_c, 10n_c, 100n_c, 300n_c$ and $500n_c$ where $n_c = m_e\omega^2/4\pi e^2$ is the critical density. We considered three types of targets composed of: (a) only electrons (immobile ions), (b) electrons and protons and (c) electrons and ions with charge $Z = 1$ having mass equal to $10m_p$ where m_p is the proton mass. Simulation box dimensions were $40\lambda \times 40\lambda$ with the mesh size $\lambda/100 =$ 10 nm.

As shown in [9, 10], electron trajectories in the standing wave demonstrate dynamic features of strange attractors at electric field nodes and loops near antinodes. As there are the different types of attractors of the dissipative electron dynamics in the CP and LP standing wave, LP seems to be more efficient for pair production in the case of the electron target.

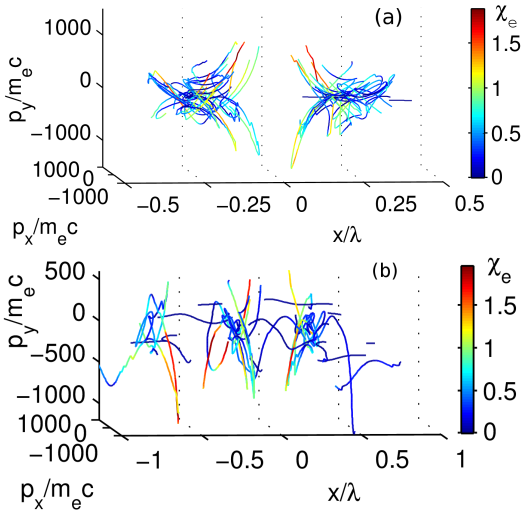

Figure 1: *Electron trajectories in the phase space during one laser period. Target of density* $100n_c$ *with (a) immobile ions and (b) with protons.*

We studied the strange attractors for wider range of different initial conditions, i. e. different types of targets, to understand how the ions affect the strange attractors and consequently pair production. In the case of LP, the highest efficiency of pair production is achieved when the target includes only electrons (i.e. immobile ions as a background), regardless on target density. In the LP case, electron trajectories show the feautre of the strange attractors at electric field nodes ($x = \pm\lambda/4$) as illustrated in Fig. 1(a). Electrons spiral to the electric field node radiating out their energy until they are again accelerated by the oscillating EM field of the standing wave. Therefore, χ_e parameter of cycling electrons periodically grows and then drops as photons are radiated.

Once protons and their space charge are considered, the structure of the strange attractors is disturbed leading to a lower pair production efficiency (Fig. 2). As seen from the trajectory plot in Fig. 1(b), more electrons propagate along the x-axis away from the interaction region, in comparison with the previous case, crossing nodes located at $x = \pm\lambda/4$ and $x = \pm 3\lambda/4$. In this case, protons start to be relativistic (for protons $a_0 \approx 0.5$). Due to the space-charge field and ponderomotive force, they oscillate also outside the nodes and escape from the interaction region, as shown in Fig. 3(a). The disturbed structure of the strange attractors leads to a less efficient pair

production despite the fact that the electrons are located at higher number of electric field nodes. When mass-to-charge ratio of ions is 10 times higher than for protons, electrons again follow trajectories at electric field nodes similarly to Fig. 1(a), i.e. the attractors of electron motion occur. As shown in Fig. 3(b), ions are concentrated at nodes $x = \pm\lambda/4$ due to the space-charge field, partially keeping the electrons here.

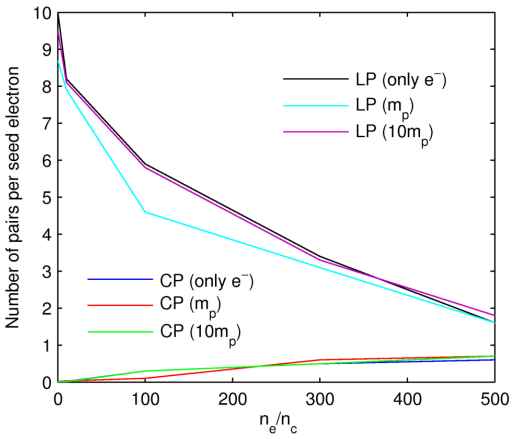

Figure 2: *Number of generated pairs per one seed electron for different types of targets and for both laser polarization.*

In Fig. 2 the pair production efficiency is shown. While pair production efficiency steadily increases for CP laser pulses, it decreases for LP. Nevertheless, the efficiency of pair production is higher for LP laser pulses in comparison with CP ones due to the strange attractors. The lower target density, the more pairs are generated in the case of LP. With increasing target density it is more difficult to establish the standing wave. Therefore, its structure is perturbed that leads to vanishing of the attractors and loops. Simulations show that even for the target of density $500n_c$, more than one pair per one seed electron is generated, i.e. the avalanche QED cascade is developed.

The role of a target density is more important than the impact of mass-to-charge ratio on pair production efficiency. Overdense targets including ions with the higher mass-to-charge ratio are more suitable for pair production. For example if the target having density $100n_c$ includes ions with mass $10m_p$ and $Z = 1$, the number of generated pairs is about 25% higher in comparison with the target containing electrons and protons.

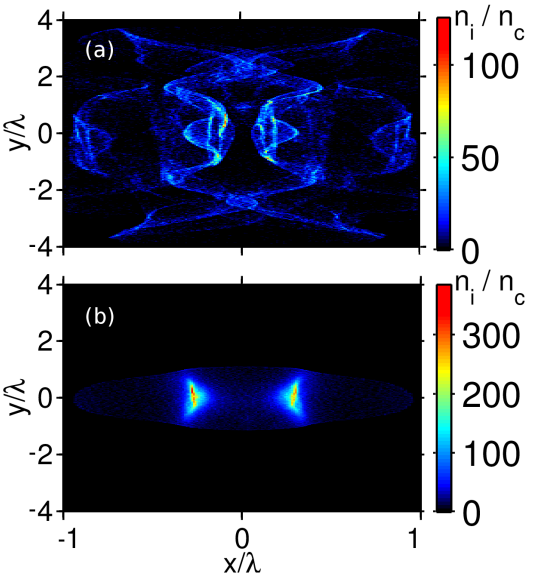

Figure 3: *Ion density n_i in case of target with initial density $100n_c$ containing (a) protons and (b) ions having mass $10m_p$.*

We also considered the interaction of laser pulses with the fully ionized aluminium target. The initial density of circular target was 2700 kg/m^3 and we used three diameters of the target: 0.5 μm, 1.0 μm, and 2.0 μm. The number of created pairs per one seed electron decreases as the target thickness grows. For LP laser pulses we obtained 3.5, 1.2, and

0.2 pairs per one seed electron, respectively. In the first case, 3% of laser pulse energy were converted into gamma radiation and pairs. For larger targets, the fraction of absorbed laser energy drops below 1% because laser pulses are partially reflected and can not penetrate into the target and establish the standing wave. Much higher absorption is expected when longer laser pulses as well as low-density targets are used [11]. The reason is that electrons oscillating in the standing wave perform more cycles at nodes and therefore emit more photons that can be converted into pairs. In the case of CP, the number of pairs generated per one seed electron was about one order of magnitude lower.

In conclusion, the role of target density and mass-to-charge ratio of ions on pair production efficiency has been assessed. It has been found that pair production is at maxmium when tenuous targets (gases) are used. Such targets allow to minimize the distortion of the standing wave so that the strange attractors can develop. Pair production efficiency grows with increasing mass-to-charge ratio of the ions in the target. In all studied cases, linear polarization of the standing wave seems to be more efficient for pair production, regardless on target density or ions included.

This research has been partially supported by the Czech Science Foundation (Project No. 15-02964S) and the Project ELI: Extreme Light Infrastructure (CZ.02.1.01/0.0/0.0/15 008/0000162) from European Regional Development.

References

[1] ELI Beamlines, www.eli-beams.eu; G. Mourou, G. Korn, W. Sandner, and J. L. Collier, ELI Whitebook (Andreas Thoss, Berlin, 2011); G. Cheriaux et al., AIP Conf. Proc. **1462**, 78 (2012); Exawatt Center for Extreme Light Studies (XCELS), www.xcels.iapras.ru.

[2] A. R. Bell and J. G. Kirk, Phys. Rev. Lett. **101**, 200403 (2008)

[3] E. G. Gelfer, A. A. Mironov, A. M. Fedotov, V. F. Bashmakov, E. N. Nerush, I. Yu. Kostyukov, N. B. Narozhny, Phys. Rev. **A 92**, 022113 (2015)

[4] V. Ritus, Journal of Soviet Laser Research **6**, 497 (1985)

[5] J. Schwinger, Phys. Rev. **82**, 664 (1951)

[6] S. S. Bulanov, T. Zh. Esirkepov, A. G. R. Thomas, J. K. Koga, S. V. Bulanov, Phys. Rev. Lett. **105**, 220407 (2010)

[7] T. D. Arber, K. Bennett, C. S. Brady, A. Lawrence-Douglas, M. G. Ramsay, N. J. Sircombe, P. Gillies, R. G. Evans, H. Schmitz, A. R. Bell, C. P. Ridgers, Plasma Phys. Controlled Fusion **57**, 113001 (2015)

[8] G. Breit, J. A. Wheeler, Phys. Rev. **46**, 1087 (1934)

[9] T. Zh. Esirkepov, S. S. Bulanov, J. K. Koga, M. Kando, K. Kondo, N. N. Rosanov, G. Korn, S. V. Bulanov, Phys. Lett. **A 379**, 2044 (2015)

[10] M. Jirka, O Klimo, S. V. Bulanov, T. Zh. Esirkepov, E. Gelfer, S. S. Bulanov, S. Weber, G. Korn, Phys. Rev. E **93**, 023207 (2016)

[11] T. Grismayer, M. Vranic, J. L. Martins, R. A. Fonseca, L. O. Silva, Phys. Plasmas **23**, 056706 (2016)